Science Advances
AAAS

advances.sciencemag.org/cgi/content/full/6/1/eaax6250/DC1

Supplementary Materials for

Growing up *Tyrannosaurus rex*: Osteohistology refutes the pygmy "*Nanotyrannus*" and supports ontogenetic niche partitioning in juvenile *Tyrannosaurus*

Holly N. Woodward*, Katie Tremaine, Scott A. Williams, Lindsay E. Zanno, John R. Horner, Nathan Myhrvold

*Corresponding author. Email: holly.ballard@okstate.edu, holly.n.woodward@gmail.com

Published 1 January 2020, *Sci. Adv.* **6**, eaax6250 (2020)
DOI: 10.1126/sciadv.aax6250

This PDF file includes:

Supplementary Materials and Methods

Geologic Setting

BMRP 2002.4.1 and BMRP 2006.4.4 were collected from latest Cretaceous (Maastrichtian) Hell Creek Formation exposures in western Carter County, Montana under BLM Permit MTM 90904 and MTM 95725. One of the most extensively studied geologic formations (e.g., *41, 42, 43*), the Hell Creek Formation records the latest Cretaceous and the K/Pg extinction event (67 – 66.052 ± 0.008 MA (*44, 45*)). The formation is found extensively in eastern Montana and the western Dakotas, and represents a fluvial system comprised of sandstones, mudstones, and clays deposited by meandering channels and floodplains draining toward the regressive Western Interior Seaway. The Hell Creek Formation can be as thin as 50 meters in southcentral North Dakota (*46, 47*), but approaches 150 meters in western Carter County, Montana (*48*).

Specimen BMRP 2002.4.1, a partially articulated small tyrannosaurid, consists of a fairly complete skull, and a skeleton over 52% complete by bone count (*49*). The locality BM2002.1 is a coarse-grained sandstone/conglomerate 12-40 centimeters in thickness overlying a weakly crossbedded point bar river deposit. The sandstone/conglomerate layer contains greenish clay clasts, small siderite concretions, fossil leaves, and pollen. The layer is interpreted as a mudflow from a flood event or overbank collapse (*49*).

Specimen BMRP 2006.4.4 represents a disarticulated but associated tyrannosaurid specimen, slightly larger than BMRP 2002.4.1. While less complete than BMRP 2002.4.1, it preserves important postcranial bones including: left scapulocoracoid, right humerus, partial ulna, manual unguals, four dorsal vertebrae, thoracic ribs, partial gastraliae, left femur, partial left fibula and tibia, several pedal phalanges, and a first digit pedal ungual.

BMRP 2006.4.4 was collected from locality 2006.2, which overlies a crossbedded point bar within a channel system. The layer containing the specimen is a medium- to coarse-grained sandstone/conglomerate also containing clay clasts. The presence of many microvertebrate fossils as well as additional dinosaur bones (e.g., disarticulated vertebrae and a *Thescelosaurus* tibia) indicate this is a lag deposit.

Taxonomic assignment

The status of BMRP 2002.4.1 as a tyrannosaurine is well established (*2, 6, 26, 50, 51*). The femur and tibia of BMRP 2006.4.4 can be referred to Tyrannosaurinae based on the following suite of morphological features (*52-54*): dorsally directed femoral head; proximal margin of the femur concave in caudal view due to dorsal elevation of greater trochanter; lesser trochanter subequal in height with greater trochanter; alariform lesser trochanter of the femur separated by a narrow cleft; lesser trochanter with deeply concave lateral aspect; deep caudolateral depression on the proximal femur bounded cranially by a vertical ridge on the lesser trochanter ($L_{1\text{-}2}$ *sensu* Brochu (*25*)) and caudoventrally by a well-developed, bulbous trochanteric crest; presence of a single intertrochanteric nutrient foramen on the proximal femur; a principle nutrient foramen located medial to the long axis of the lesser trochanter on the proximal femoral shaft; pronounced accessory trochanter; fourth trochanter distally positioned (40% of femoral length); slightly concave caudal aspect of the femoral shaft in the region of the fourth trochanter; overlap between the fourth and lesser trochanters; circular scar on caudal aspect of femur abuts medial margin of shaft; a lens-shaped cross-section of the distal femur exhibiting pronounced mediodistal and ectepicondylar crests; crista tibiofibularis restricted to medial half of lateral condyle; a dorsally elevated cnemial crest of the proximal tibia; and an accessory condyle extending from lateral condyle of the proximal tibia (fig. S1).

Histology Descriptions of BMRP 2002.4.1 and BMRP 2006.4.4

BMRP 2002.4.1

Femur, transverse section:

The femur of BMRP 2002.4.1 is partial and fragmentary (fig. S2A). Transverse sections were made for a previous study from two diaphyseal pieces labelled Fe1-1 and Fe1-3. The original orientation and location of each fragment about the diaphysis cannot be determined.

Fe1-1: From inner to outer cortex, primary tissue is a woven-parallel complex and vascularity is longitudinal, laminar, and sub-plexiform (fig. S3A). Viewed in circularly polarized light (CPL), the concentric lamellae comprising the sub-plexiform and many longitudinal primary osteons are anisotropic, corresponding to transversely-oriented lamellar mineralized fibers in primary osteons. In some cases, however, primary osteons are uniformly isotropic except in the region immediately adjacent to vascular canals, which is anisotropic (fig. S3B). This change in birefringence from isotropic to anisotropic within a primary osteon indicates a change in fiber orientation during formation. The isotropic regions of primary osteons are most likely due to the arrangement of lamellar mineralized fibers perpendicular to the plane of section (*14*), opposed to a parallel orientation to plane of section. Evidence for this perpendicular arrangement of fibers can be seen in plane polarized light (PPL), where the mineralized fibers surrounding correspondingly isotropic primary osteons have a "bubbly" appearance, indicative of mineralized fiber bundles viewed in transverse (perpendicular) section (fig. S3C). Osteocyte lacunae within these isotropic primary osteons are also rounded in shape, likely due to having been sectioned through their minimum axis.

Noticeable anisotropy is observed on a regional scale (fig. S3A). Locally, the primary tissue laminae between osteons is a combination of isotropic and anisotropic fibers (fig. S3B), suggesting a weakly woven to poorly organized parallel-fibered matrix. Osteocyte lacuna density is high and lacunae are somewhat flattened in anisotropic regions, while more rounded in isotropic areas. Lacunae are noticeably flattened in the largely avascular regions adjacent to cyclical growth marks (CGMs; includes annuli and lines of arrested growth), where mineral fibers are also more anisotropic.

Fe1-3: Primary tissue and vascular organization is similar to thin section Fe1-1. However, this thin section fragment includes a column of dense Haversian tissue from inner to outer cortex indicative of a tendon attachment site.

Tibia, transverse section:

The right tibia of BMRP 2002.4.1 (figs. S2B and S4) lacks a lamellar endosteal layer but it is unclear whether it lacked one in life or whether the endosteal layer broke off post-burial or possibly during preparation. Throughout, primary tissue is of a woven-parallel complex, varying locally in vascular canal orientation. CPL reveals that longitudinal primary osteons are isotropic and contain rounded osteocyte lacunae (see Fig. 2A), but laminar, circular, and plexiform primary osteons are anisotropic with flattened osteocyte lacunae. The laminae between primary osteons is a combination of isotropic and anisotropic fibers with plump osteocyte lacunae regardless of fiber orientation, which together suggests a poorly organized parallel-fibered, or somewhat woven, matrix (see Fig. 2A and B). The thickest cortex (16 mm) is located

anteromedially (fig. S4A). Within the innermost cortex of the anteromedial and medial sides, there is a sparse scattering of small (~145 microns in diameter) isotropic secondary osteons and vascularity is primarily longitudinal to laminar (fig. S4B). More posteriorly, vascularity is also longitudinal to laminar. The thinnest cortex (10 mm) spans the posterolateral, anterolateral, and anterior sides (fig. S4A). On the lateral side, circular and plexiform vascularity dominates (fig. S4C), becoming laminar and longitudinal in the anterolateral cortex (fig. S4D).

Anterolaterally, there is an isolated region spanning the inner to outer cortex consisting of isotropic Haversian systems, likely associated with tendon attachment and tension loading (*14*) (fig. S4D and E). At high magnification, the isotropic secondary osteons appear "bubbly" in transverse section under PPL (fig. S4F). This appearance is likely due to viewing mineralized parallel fiber bundles cut perpendicular to their long axis orientation, like the lamellae comprising isotropic primary osteons. The CGMs are most widely spaced relative to each other in the medial and posterior cortex, and most closely spaced in the lateral cortex, indicating posteromedial directional cortical growth prior to death (fig. S4G and H).

Tibia, medial-lateral longitudinal section:

Throughout the longitudinal section (fig. S5 and Fig. 2B), osteocyte lacunae are so dense that the bone appears fibrous (fig. S5B). Within the laminae, there are localized regions of isotropic and anisotropic tissue, with osteocyte lacunae ranging in shape from rounded to flattened; these observations confirm the poorly organized parallel-fibered to weakly woven nature of the primary laminae. Adjacent to the longitudinal vascular canals, the tissue comprising primary osteons is anisotropic in CPL with longitudinally flattened osteocyte lacunae (fig. S5B – D and Fig. 2B), confirming the source of osteon isotropy when viewed in the transverse plane. CGMs are difficult to distinguish in longitudinal section.

On the medial side within the innermost cortex, vascular canals are arranged haphazardly to the plane of section with numerous connections from Volkmann's canals (fig. S5B). From mid to outer cortex, the vascular canals course vertically (proximal-distal), with fewer transverse communicating canals (fig. S5C), corresponding to the circular vascular orientation observed in transverse section. Here, lamina thickness between primary osteons is ~67 µm.

As noted previously, the lateral cortex is thinner than that of the medial cortex (fig. S5A). Throughout the lateral cortex, osteocyte density is high but less so than the medial side. Laminae between vascular canals is also thinner than on the medial side (~56 µm), and canals are uniformly vertical with few transverse communications (fig. S5D).

BMRP 2006.4.4

Femur, transverse section:

In transverse section (figs. S2C and S6A), the left femur of BMRP 2006.4.4 appears regionally anisotropic. Locally, however, fiber orientation varies between isotropic and anisotropic fibers, although the degree of anisotropic fibers varies about the cortex. Within primary tissue laminae, the dense osteocyte lacunae vary in shape from flattened within the anisotropic fibers to round within isotropic fibers (see Fig. 1B). Vascular canal orientation also varies locally about the cortex. In most cases, primary osteons surrounding vascular canals are highly isotropic, save for the anisotropic lamellae adjacent to the vascular canal (see Fig. 1B). Cortical thickness is fairly uniform, but somewhat thicker on the medial side (~16.9 mm) than the lateral side (~14.2 mm) (fig. S6A). A lamellar endosteal layer (fig. S6B) separates previously eroded innermost cortex

from the medullary cavity, although in places it appears to have broken away post-burial and is not present. Isotropic primary tissue with dense rounded osteocyte lacunae are found on the medullary surface of the lamellar endosteal layer on the anterior and posterolateral sides of the cortex. This unusual tissue is mentioned for descriptive completeness, but is intentionally not figured as it is currently under study.

Within the innermost cortex of the anteromedial side there is a sparse scattering of secondary osteons. Vascular canal orientation is longitudinal to laminar and becomes a combination of laminar and sub-plexiform from mid- to outer cortex (fig. S6B). On the medial and posteromedial sides, vascular canals are longitudinal and laminar, with a higher proportion of longitudinal canals towards the outer cortex. There is an annulus at the periosteal surface on the medial side, where osteocyte lacunae are flattened, and lacuna density and vascular canal density are reduced (fig. S6C; Fig. 1D). There is a dense column of isotropic secondary osteons from inner to outer cortex beginning on the posteromedial side and continuing posteriorly, characteristic of a tendon attachment site and tension loading (*14*) (fig. S6C).

The innermost cortex of the posterior side was damaged, and only the outermost cortex was preserved for description (fig. S6A). Posterolaterally and laterally, multiple generations of isotropic secondary osteons comprise the innermost cortex. Interstitially, vascular canal orientation is laminar to plexiform within the inner to mid-cortex. From outer cortex to the periosteal surface, vascular canal arrangement alternates in thick bands of laminar primary osteons and those of longitudinal to reticular primary osteons (fig. S6D). The bands containing longitudinal and reticular primary osteons have a matrix of isotropic laminae. Each band of primary tissue is separated by a CGM. The annulus located at the periosteal surface observed on the medial side (fig. S6C) occurs within the outer cortex as a thick avascular region with flattened osteocyte lacunae (fig. S6D see also Figs. 1D and E). It is followed by cortex to the periosteal surface comprised of uniformly isotropic fibers with reticular vascular canals and a high density of round osteocyte lacunae.

As with the posterior side, there is a column of secondary osteons from inner to outer cortex on the lateral side characteristic of a region of tendon attachment. Interstitial primary tissue and vascularity resembles that of the posterolateral side. Here the annulus is again at the periosteal surface, but thins and disappears when followed anteriorly. On the anterolateral side, osteocyte lacunae are dense from inner to outer cortex and vascular canal orientation is uniformly longitudinal and laminar (fig. S6E). There is a scattering of secondary osteons within the innermost cortex. On the anterior side there is another column of secondary osteons indicating a tendon attachment site.

Femur, posteromedial-anterolateral longitudinal section:

In longitudinal section, the anterolateral cortex of BMRP 2006.4.4 is thinner than the posteromedial cortex (figs. S2C, S6A, and S7A), but they are otherwise identical in tissue and vascular organization. In general, osteocyte lacuna density is high, and vascular canals are straight in a proximal to distal orientation, with occasional transverse Volkmann's canal communications. Adjacent to the longitudinal vascular canals, mineralized fibers are highly anisotropic in CPL, with longitudinally flattened osteocyte lacunae. This confirms that primary osteons are comprised of longitudinally-oriented parallel-fibered tissue, which appeared isotropic with round osteocyte lacunae in transverse section (see Fig. 1B and C). Laminae between primary osteons vary in isotropy, with osteocyte lacunae ranging in shape between rounded and

flattened, corresponding to the weakly parallel-fibered orientation in transverse plane (see Fig. 1C). CGMs are frequently challenging to distinguish in longitudinal plane, but some are more evident than others, appearing as thin isotropic vertical lines in CPL (fig. S7B). In principle, CGMs in longitudinal plane should be the same distance from the periosteal surface as they are in transverse plane. However, the longitudinal section reveals that CGMs are not perfectly vertical, but are angled; as a CGM represents the periosteal surface during a pause or decrease in growth, they reveal the cortical shape in longitudinal view during each annual hiatus (fig. S7B). In addition, the medial cortex reveals a band of primary osteons traveling diagonally through the cortex, moving from inner cortex at the proximal side to outer cortex on the distal side (fig. S7). Possibly this band of tissue is related to an ontogenetically migrating region of reticular vascularity, tendon enthesis, or change in diaphyseal shape.

Tibia, transverse section:

Because only the proximal portion of the left tibia was recovered from the 2006.2 locality, the sample removed for thin section processing was not located at the minimum circumference of the diaphysis and therefore incorporates the fibular crest (fig. S2D and S8A). The primary cortex is of a woven-parallel complex, with vascular canal orientation varying locally. Primary osteons are frequently isotropic in CPL, regardless of vascular orientation. Osteocyte lacuna density is high and varies between round and compressed within the cortex. Aside from the region of the fibular crest, the cortex on the lateral, medial, and posterior sides is fairly uniform in thickness, ranging between 11 mm and 13 mm. The cortex is thickest on the anterior side (~ 18 mm). The entire cortex is separated from the medullary cavity by a lamellar endosteal layer (fig. S8B). On the anterior and anterolateral sides, the endosteal layer gives rise to a tissue with low birefringence and high longitudinal and reticular vascularity with rounded and dense osteocyte lacunae, similar to the endosteal tissue described above in the femur of BMRP 2006.4.4. A continuous endosteal layer indicates that no medullary expansion was actively occurring at time of death. However, directional rapid periosteal cortical growth is evident by the highly vascularized, reticular tissue present at the periosteal surface on the anterolateral, anterior, and anteromedial sides (see Fig. 2C). Vascularity of the anterolateral side is largely laminar, circular, and plexiform. Beginning within the mid-cortex on the anterolateral side, three zones of primary tissue bounded on either side by CGMs consist of highly isotropic fibers with reticular vascular canals (fig. S8C). Within these zones on the anterior side, the primary tissue is almost completely replaced by secondary osteons (fig. S8D).

Secondary osteons are frequent within the innermost cortex on the anterolateral and anterior sides. Here, five zones are noticeably compressed between 6 LAGs (see Fig. 2D), suggesting minimal annual directional growth when the individual was younger if each CGM is considered either to represent an annual hiatus, or a single year of sporadic growth. Because of the proximal sampling locality, the potential interference of the fibular crest on bone shape, and absence of this LAG stacking in the associated femur, we conservatively consider this to be a single event. Histological examination of the associated fibula may provide interpretive clarification if the LAGs are present.

Anteromedially, the innermost cortex was eroded by medullary drift earlier in life, which truncated the innermost CGMs. In this area, secondary osteon density is high but primary tissue is visible interstitially (see Fig. 2D). Secondary osteons are frequent mid-cortex but are sparsely scattered in the outer cortex.

Vascularity is laminar to sub-plexiform throughout on the medial side. Secondary osteons are scattered, but more frequent in the innermost cortex. Some groupings of secondary osteons are linearly arranged and radiate into the mid-cortex. Posteromedially, vascular canals are mostly laminar but with some radial canals (fig. S8B). While the lamellar endosteal layer is quite thin elsewhere (~180 µm), the lamellar endosteal layer is up to 755 µm thick on the posteromedial side. Here radial vascular canals are present within the endosteal layer (fig. S8B), as observed in other dinosaurs and modern birds (see Woodward et al. (*55*) and references therein). On the posterior and posterolateral sides, vascular canal orientation is longitudinal to laminar within the inner cortex, and becomes a combination of laminar to reticular from mid- to outermost cortex. This change to reticular vascularity suggests increased osteogenesis prior to death. There is an annulus at the periosteal surface on the posterolateral side of the cortex (fig. S8E), but it blends with and disappears at the periosteal surface laterally.

Cortex on the lateral side is largely comprised of Haversian systems associated with the fibular crest. Towards the anterior side of the crest, primary tissue contains radially-oriented primary osteons. Within the fibular crest there are secondary osteons and large erosional cavities lined with endosteal bone (fig. S8F). From lamellar endosteal layer to periosteal surface, the cortical region containing the fibular crest has a maximum thickness of 27 mm.

Supplementary Materials Figures

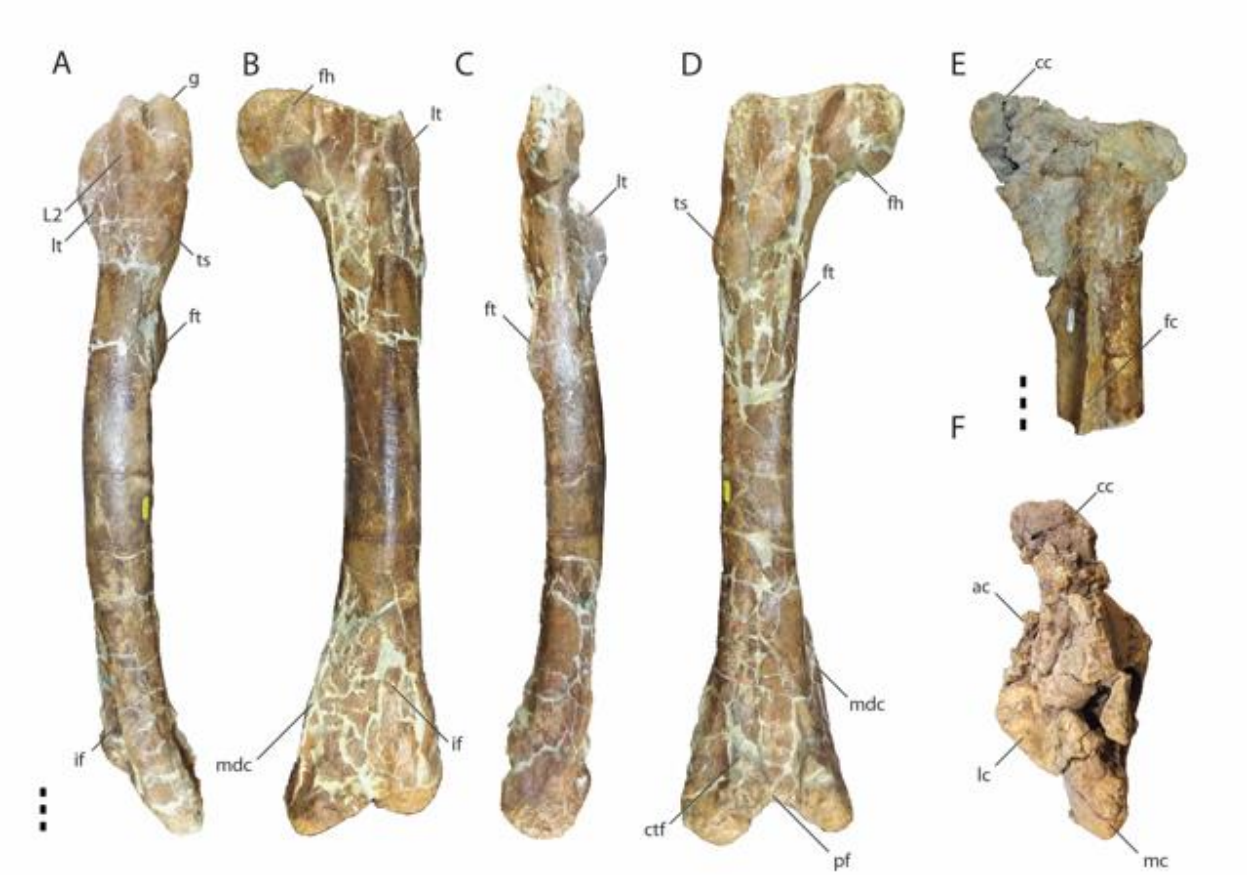

Fig. S1. Hind limb elements of BMRP 2006.4.4. Left femur in (**A**) lateral, (**B**) cranial, (**C**) medial, and (**D**) caudal views. Proximal portion of left tibia in (**E**) lateral and (**F**) proximal views. Abbreviations: ac, accessory lateral condyle; cc, cnemial crest; ctf, crista tibiofibularis; fc, fibular crest; fh, femoral head; ft, fourth trochanter; g, greater trochanter; if, intercondylar fossa; L2, lobe on lesser trochanter; lc, lateral condyle; lt, lesser trochanter; mc, medial condyle; mdc, mesiodistal crest; pf, popliteal fossa; ts, trochanteric shelf. Scale bar 5 cm. (F) not to scale.

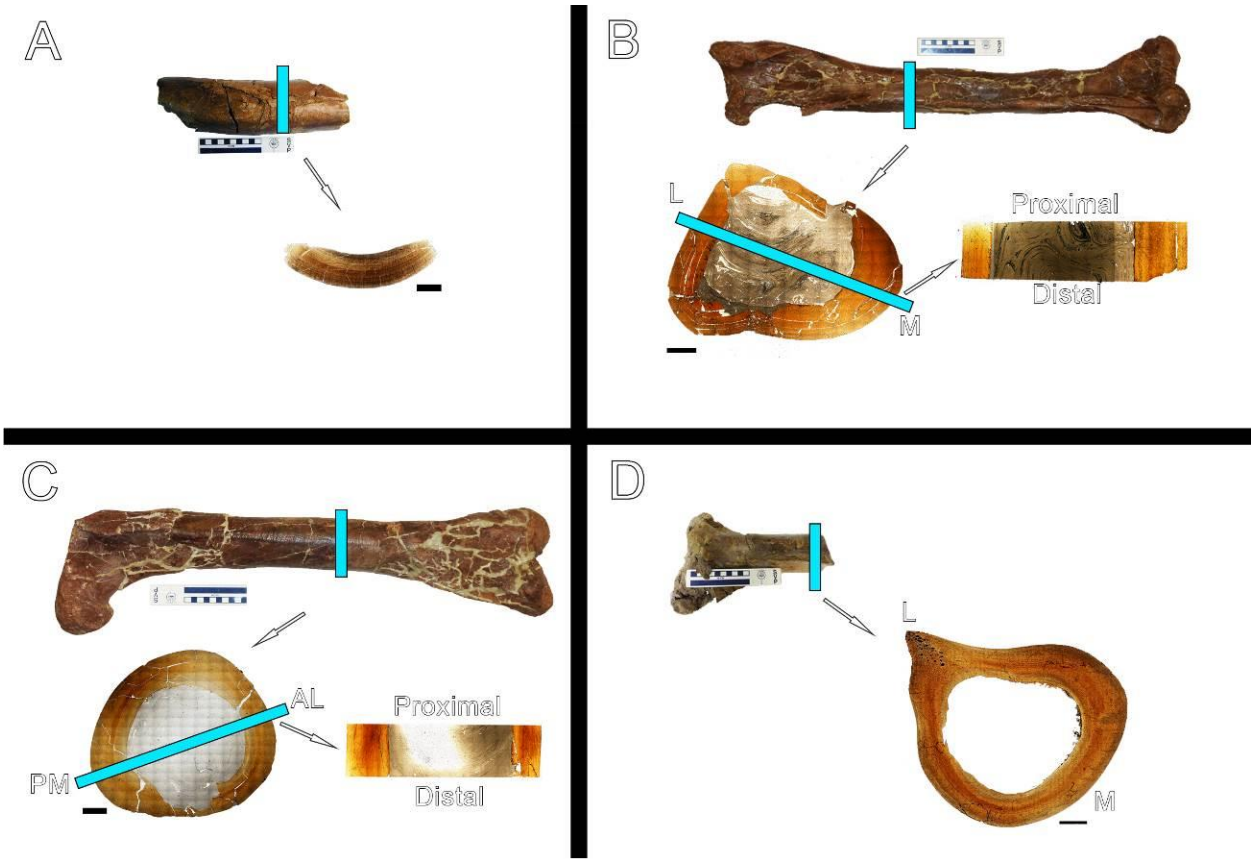

Fig. S2. Femur and tibia histology overview of tyrannosaurid specimens BMRP 2002.4.1 and BMRP 2006.4.4. (**A**) Top: the fragmentary femur of BMRP 2002.4.1 was transversely sectioned (blue line). Scale bar, 10 cm. Bottom: the resulting thin section is incomplete. Scale bar, 1 cm. (**B**) Top: the right tibia of BMRP 2002.4.1 was transversely sectioned (blue line). Scale bar, 10 cm. Left: the resulting complete transverse thin section. The embedded material was also sectioned longitudinally along a lateral (L) – medial (M) transect (blue line) to produce a longitudinal thin section. Scale bar, 1 cm. Right: the resulting longitudinal thin section. (**C**) Top: the left femur of BMRP 2006.4.4 was transversely sectioned (blue line). Scale bar, 10 cm. Left: the resulting complete transverse thin section. The embedded material was also sectioned longitudinally along an anterolateral (AL) – posteromedial (PM) transect (blue line) to produce a longitudinal thin section. Scale bar, 1 cm. Right: the resulting longitudinal thin section. (**D**) Top: the partial left tibia of BMRP 2006.4.4 was transversely sectioned (blue line). Scale bar, 10 cm. Bottom: the resulting complete transverse thin section, which incorporates the lateral crest. Scale bar, 1 cm.

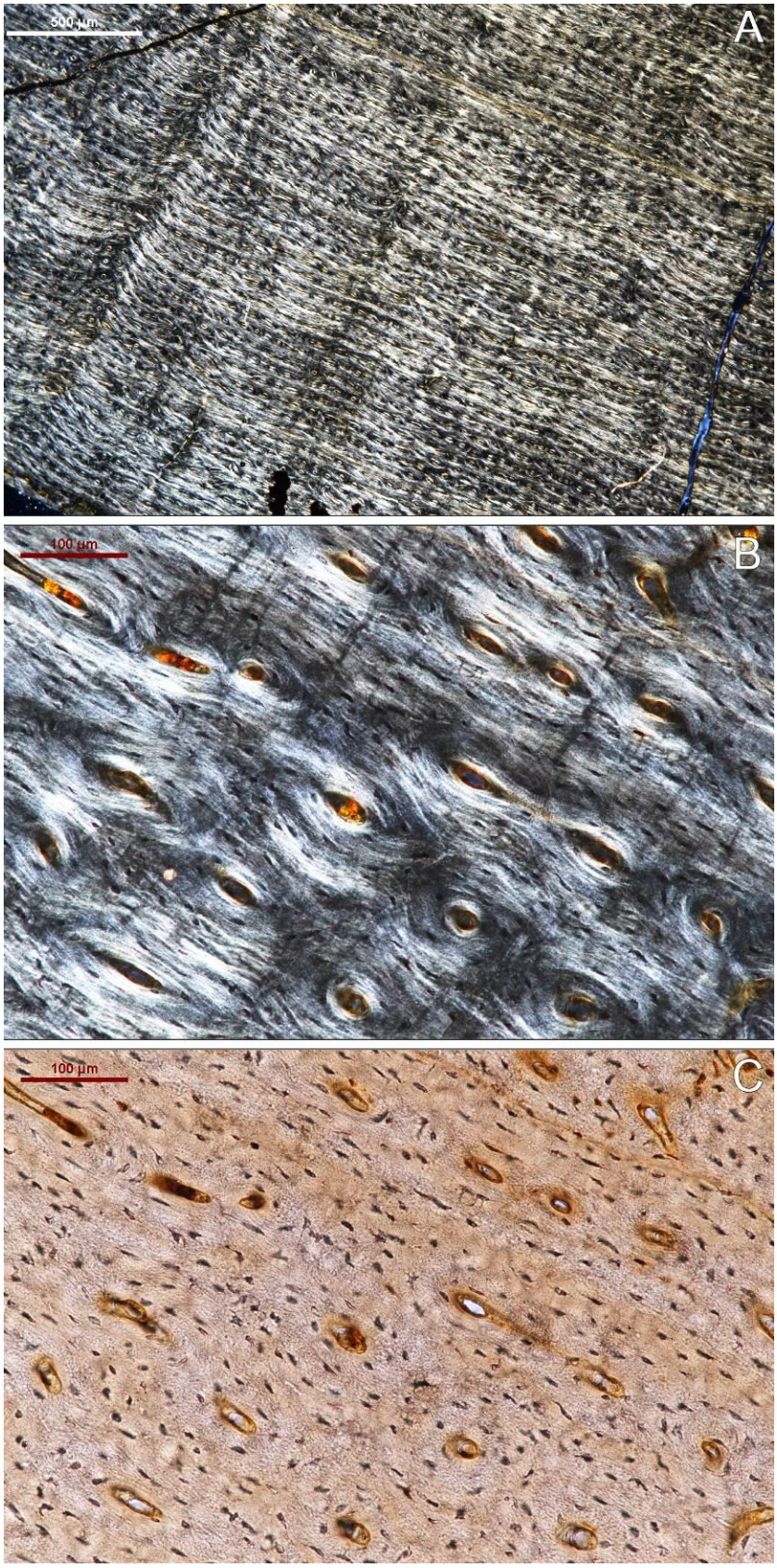
500 µm
A
100 µm
B
100 µm
C

Fig. S3. Fragmentary femur transverse thin section of BMRP 2002.4.1. (**A**) Mid- to outer cortex in CPL, with the periosteal surface at the bottom left of the image. The rich vascular network shown here is comprised of longitudinal vascular canals within a woven-parallel complex of primary tissue. Many primary osteons display isotropic lamellae encircling the vascular canals. (**B**) Magnified region of femur cortex in CPL. Regional anisotropy gives way to varying birefringence and osteocyte lacuna shape within the laminae surrounding primary osteons suggesting weakly woven or poorly organized parallel-fibered tissue. Regions of uniform isotropy within primary osteons in (B) appear "bubbly" in (**C**) with PPL because the fiber bundles are arranged perpendicular to the plane of section. CPL = circularly polarized light, PPL = plane polarized light.

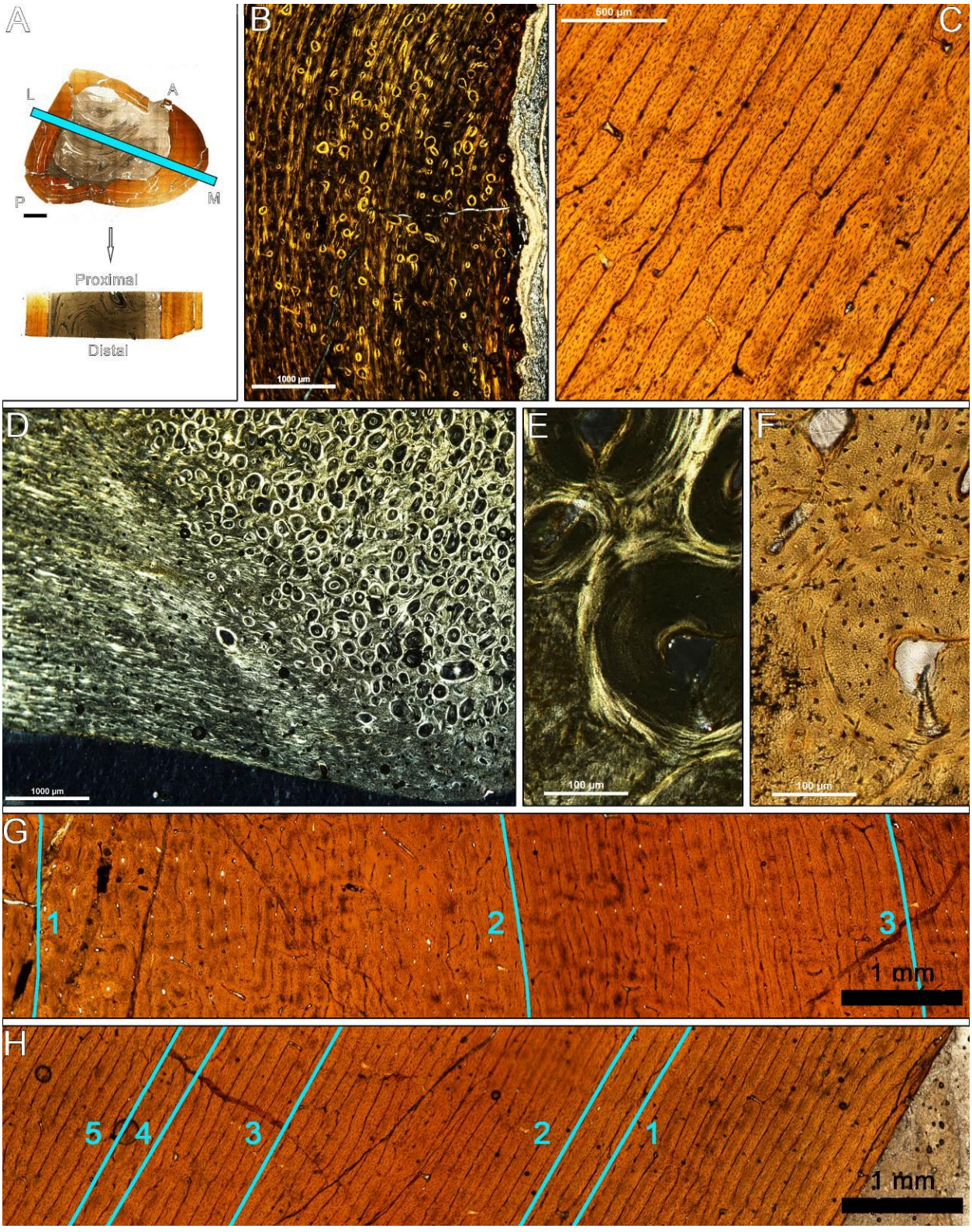
A
L
A
P
M
Proximal
Distal
B
1000 µm
C
500 µm
D
1000 µm
E
100 µm
F
100 µm
G
1
2
3
1 mm
H
5
4
3
2
1
1 mm

Fig. S4. Transverse thin section histology of the right tibia of BMRP 2002.4.1. (**A**) Transverse and longitudinal thin sections were produced from the right tibia of BMRP 2002.4.1. (**B**) In CPL the innermost cortex of the anteromedial side shows a primary cortex with longitudinal and laminar vascularity as well as a scattering of secondary osteons. The cementing lines bounding secondary osteons are highly birefringent, but secondary osteon lamellae are isotropic. (**C**) Vascularity becomes circular to plexiform on the lateral side, shown in PPL. (**D**) Anterolaterally, primary tissue gives way to a column of Haversian systems radiating from inner to outer cortex, likely associated with tendon insertion. Viewed in CPL, these secondary osteons are also isotropic. (**E**) Magnified view of anterolateral isotropic secondary osteons. When viewed in PPL (**F**), the same isotropic regions of the secondary osteons appear "bubbly", likely due to the longitudinally parallel arrangement of mineralized fibers. (**G**) Relative zonal spacing between CGMs (highlighted in blue and numbered from earliest to latest) is greater on the medial side than (**H**) the lateral side, accounting for the thicker cortex posteromedially. Increased zonal spacing posteromedially corresponds to more apposition occurring annually on the medial side relative to the lateral side prior to death. (G) and (H) shown in PPL. CPL = circularly polarized light, PPL = plane polarized light, CGM = cyclical growth mark.

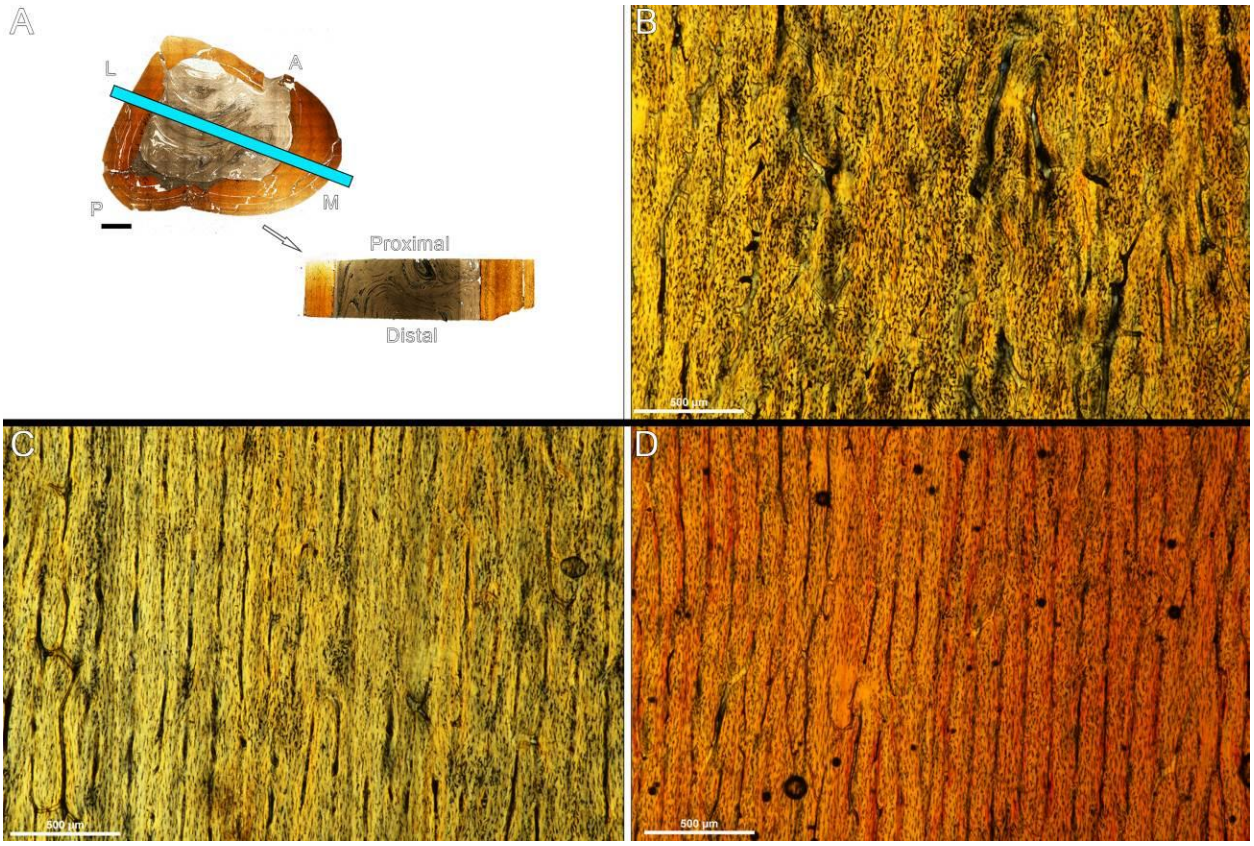

Fig. S5. Longitudinal thin section of BMRP 2002.4.1 tibia. (**A**) The tibia of BMRP 2002.4.1 was cut longitudinally along a medial – lateral transect (blue line) resulting in a longitudinal thin section (lower right). (**B**) Throughout the cortex, osteocyte lacunae are so dense they cause the thin section to appear fibrous. Magnification of the inner cortex on the medial side shows randomly organized vascular canals with frequent Volkmann's canals. (**C**) Within the mid- to outer cortex, vascular canals are vertically oriented proximal to distal, with fewer Volkmann's canals. (**D**) On the lateral side, osteocyte lacuna density is somewhat less than the medial side. Vascular canals are vertically arranged in longitudinal thin section throughout the lateral cortex.

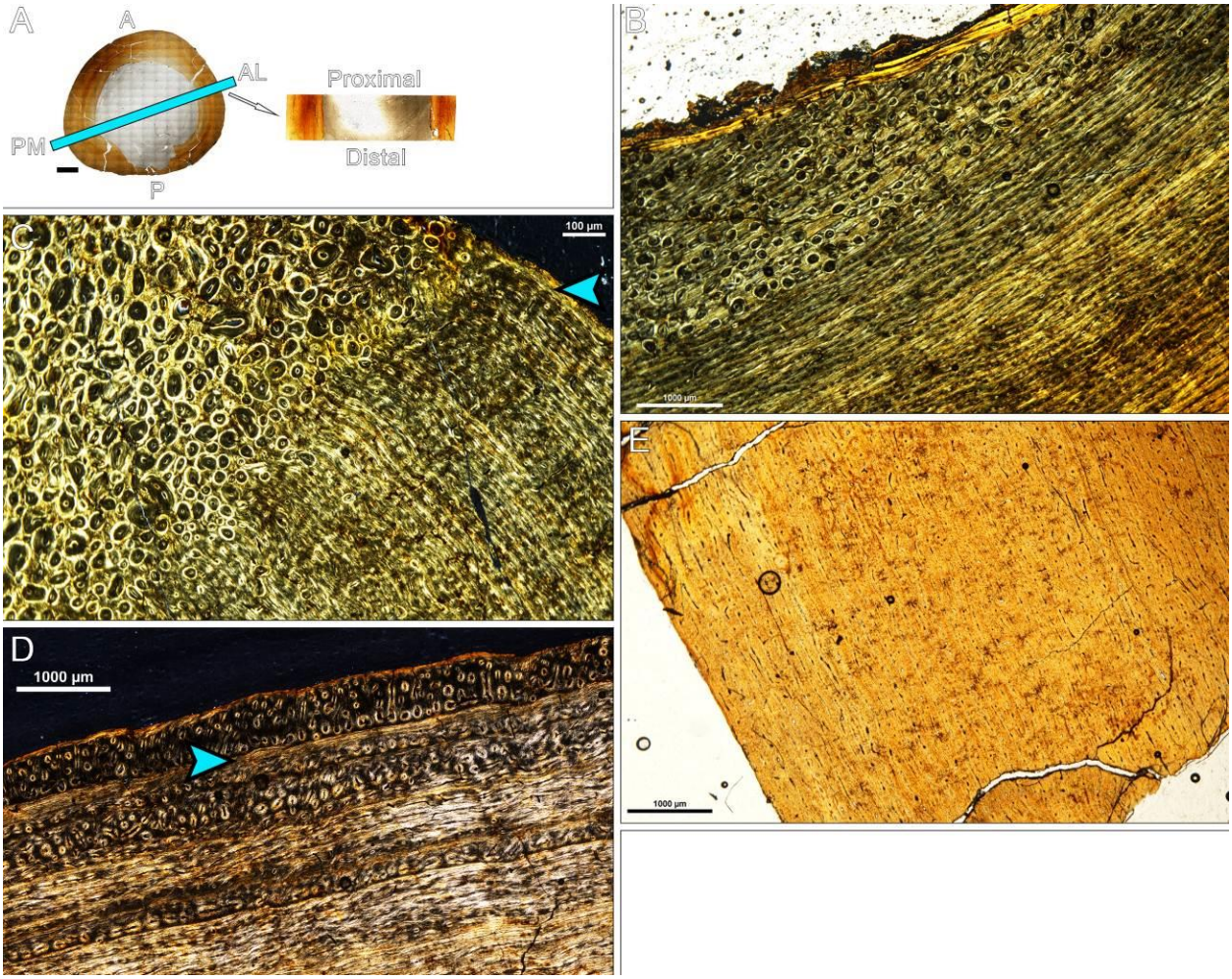

Fig. S6. Transverse and longitudinal thin sections were produced from the left femur of BMRP 2006.4.4. (**A**) The complete transverse thin section of the femur. A longitudinal thin section was also made along an anterolateral – posteromedial transect, which captures the thickest region of cortex. (**B**) A lamellar endosteal layer (top of image) separates the innermost cortex from the medullary cavity, except where it was broken off post-burial. This anteromedial view of the inner cortex shows a sparse scattering of secondary osteons and longitudinal to laminar vascularity. Image shown in CPL, with endosteal surface on the upper left. (**C**) There is a column of secondary osteons radiating from inner to outer cortex on the posteromedial and posterior sides, likely associated with tendon attachment. The annulus at the periosteal surface beginning on the medial side continues on the posterior side and is visible at the surface in the upper right of the CPL image (arrow). A column of secondary osteons is also present on the lateral and anterior sides of the cortex. (**D**) The annulus visible at the periosteal surface medially and posteriorly is within the outer cortex (arrow) on the posterolateral side, followed by longitudinal and reticular primary osteons within a regionally isotropic matrix. Within the outer cortex, there are several bands of tissue alternating between laminar primary osteons and a combination of longitudinal to reticular primary osteons. Each band is separated by a CGM. Image shown in CPL. (**E**) The anterolateral side shown in PPL consists of longitudinal and laminar vascular canals in primary tissue, with dense osteocyte lacunae and no annulus at the

periosteal surface. CPL = circularly polarized light, PPL = plane polarized light, CGM = cyclical growth mark.


A
5000 µm
B
5000 µm

Fig. S7. Longitudinal thin section of the left femur from BMRP 2006.4.4. (**A**) The longitudinal section was taken along an anterolateral – posteromedial transect, shown in CPL. The medullary cavity is filled with Apoxie Sculpt clay adhesive. On the posteromedial side of cortex, a band of primary osteons of nearly uniform thickness (blue arrow) travels through the cortex, moving from innermost cortex at the proximal end of the section (top of image) to outermost cortex at the distal end of the section (bottom of image). Possible CGMs are observed traveling from proximal to distal through the cortex, but their paths are not vertical and tend to "drift". (**B**) Enlargement of mid- to outer cortex on the posteromedial side showing the band of secondary osteons (blue arrow), as well as the most evident of possible CGMs (white arrows).

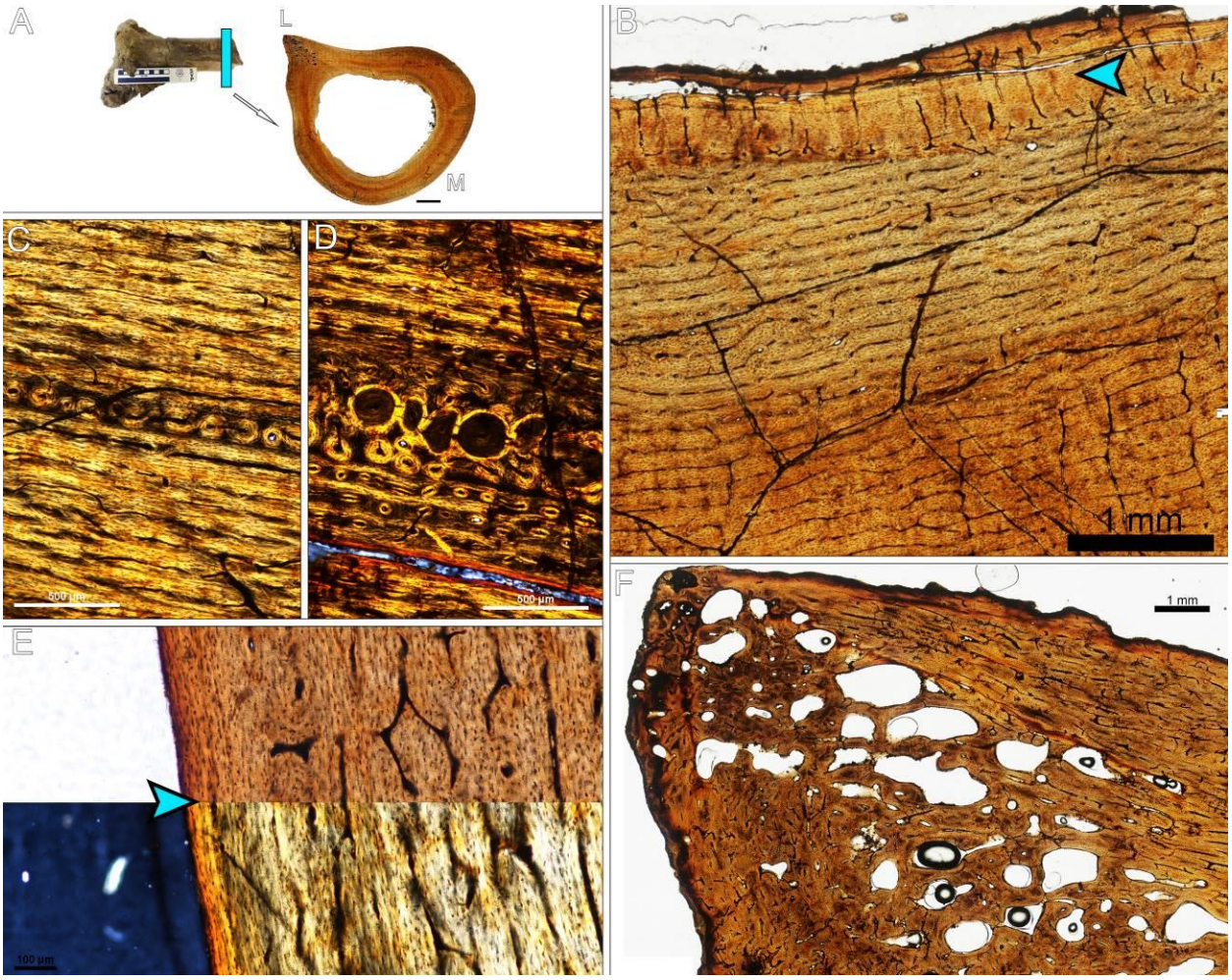

Fig. S8. Transverse thin section of the left tibia of BMRP 2006.4.4. (**A**) Only the proximal end of the left tibia was preserved, so that the transverse thin section incorporates the fibular condyle. (**B**) The continuous lamellar endosteal layer is thickest on the posteromedial side (blue arrow), and contains radial vascular canals. The cortex on the posteromedial side is primarily laminar, with scattered radial canals (visible in lower right of image). PPL. (**C**) On the anterolateral side, the majority of primary tissue is laminar, circular, and plexiform, but vascularity in three zones becomes exclusively reticular. CPL. (**D**) Following the reticular zones of tissue to the anterior side, the majority of the cortex within those zones is replaced by secondary osteons. CPL. (**E**) An annulus (blue arrow) is visible at the periosteal surface on the posterolateral side, here shown in PPL (top) and CPL (bottom). (**F**) Histology of the lateral fibular condyle. Primary tissue on the anterolateral side was growing radially, and primary osteons in this region are parallel to the transverse plane of section. The center of the fibular condyle consists of large erosion rooms bounded by lamellar endosteal layers. PPL. CPL = circularly polarized light, PPL = plane polarized light.